Photochemistry and Photobiology, 2011, 87: 329–334

Differential Impacts of Solar UV Radiation on Photosynthetic Carbon Fixation from the Coastal to Offshore Surface Waters in the South China Sea

Gang Li[1,2], Kunshan Gao*[1] and Guang Gao[1]

[1]State Key Laboratory of Marine Environmental Science, Xiamen University, Xiamen, Fujian, China
[2]Key Laboratory of Marine Bio-resources Sustainable Utilization, South China Sea Institute of Oceanology, CAS, Guangzhou, Guangdong, China

Received 25 October 2010, accepted 14 November 2010, DOI: 10.1111/j.1751-1097.2010.00862.x

ABSTRACT

We carried out experiments during an expedition (14 August to 14 September, 2007) that covered up to 250 000 km^2 to investigate the effects of solar UV radiation (UVR, 280–400 nm) on the photosynthetic carbon fixation of tropical phytoplankton assemblages in surface seawater of the South China Sea. From coastal to pelagic surface seawaters, UV-B (280–315 nm) caused similar inhibition, while UV-A (315–400 nm) induced photosynthetic inhibition increased from coastal to offshore waters. UV-B resulted in an inhibition by up to 27% and UV-A by up to 29%. Under reduced levels of solar radiation with heavy overcast, UV-A resulted in enhanced photosynthetic carbon fixation by up to 25% in coastal waters where microplankton was abundant. However, such a positive impact was not observed in the offshore waters where piconanoplankton was more abundant. The daily integrated inhibition of UV-A reached 4.3% and 13.2%, and that of UV-B reached 16.5% and 13.5%, in the coastal and offshore waters, respectively.

INTRODUCTION

Marine photosynthetic organisms play an important role in the oceanic biological CO_2 pump. Within the euphotic zone, phytoplankton cells utilize photosynthetically active radiation (PAR, 400–700 nm) to drive photosynthesis; however, the cells in the upper part of this layer are also exposed to ultraviolet radiation (UVR, 280–400 nm) that can penetrate up to 60 m into the pelagic water column (1). Since the ozone depletion in the Antarctic and other latitudes, more and more attention has been paid to the effects of UVR on the processes involved in primary production (2). Solar UV-A (315–400 nm) or/and B (280–315 nm) can reduce growth and photosynthetic rates (3,4), increase permeability of cell membranes (5), damage proteins (6) or DNA molecules (7–9), and even lead to cell death (10). On the other hand, UV-A can aid in photorepair of UV-damaged DNA (11) and enhance carbon fixation under reduced levels of solar radiation (12–14) or fast mixing conditions (15,16). Furthermore, UV-A appears to be used in photosynthesis of algae in the absence of PAR (14,17).

Spatial variations in phytoplankton biomass and taxonomic structure from coast to pelagic waters have been well-documented (3,18,19). Coastal waters are usually nutrient-rich (20,21), whereas open oceans are often oligotrophic and thus less productive due to nutrient limitation (22,23). Microplankton (>20 μm) are more plentiful in coastal waters (21); while picoplankton (<2 μm) are more abundant in open oceans (19). In terms of their responses to UVR, large-cells are capable of synthesizing and accumulating UV-absorbing compounds (UVACs) that play a protective role against UVR; these screening compounds are not found in picoplankton cells (24,25). Therefore, picoplankton cells can be more sensitive to solar UV, although their repair process of damaged-DNA is much faster (7,26). Since the taxonomic composition, accumulation of UV-absorbing compounds and nutrient availability are typically different, physiological responses of phytoplankton assemblages to solar UV can differ geographically from coastal to pelagic waters. However, little is known about the differential effects of UV on marine primary production among the geophysical marine environments.

The South China Sea (SCS) is notable for its shallow mixed layer (<50 m), low nutrients levels (below detection limits) and high light transparency (27,28). Phytoplankton cells in SCS can thus be exposed to higher irradiances and doses of solar radiation, compared with other ecosystems that are located at higher latitudes (29). Recently, the photobiological responses of phytoplankton assemblages to solar UV have been examined in the coastal water of the SCS (13,14,16,30,31). However, little is known about the open waters. Here, we have shown the effects of UVR on the photosynthetic carbon fixation of natural phytoplankton assemblages in SCS, with special reference to their spatial variations from coast toward open oceans.

MATERIALS AND METHODS

Study area and sampling protocol. This study was carried out during a cruise (11-15ºN, 109-114ºE) of 32 days (August 14 to September 14, 2007) in the SCS (Fig. 1). The cruise covered approximately 250 000 km^2 with depth ranging from about 300 to 3000 m from coastal to pelagic waters. Surface seawater (within 30 cm depth) was collected at 8:30 A.M. every morning with a 1.3 L acid-cleaned (1 M HCl) polycarbonate carboy. Incubation for photosynthetic carbon fixation by the phytoplankton assemblages was initiated within 15 min after the collection.

*Corresponding author email: ksgao@xmu.edu.cn (Kunshan Gao)

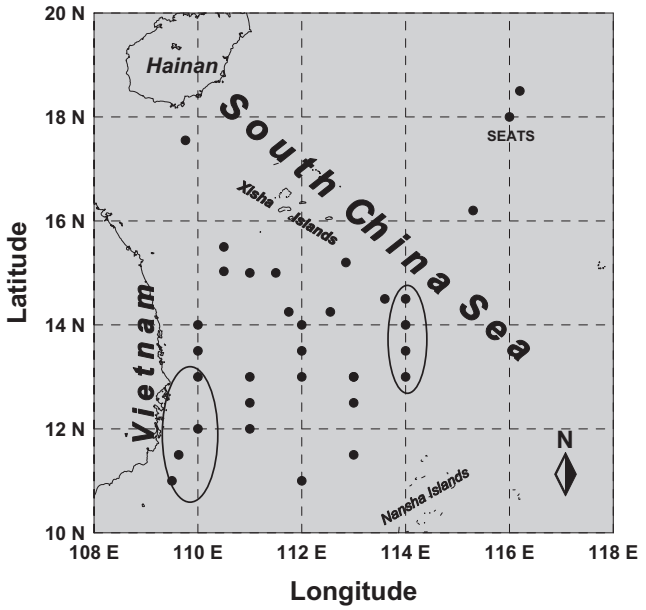

Figure 1. Sampling sites (solid circles) during the cruise dated from 14 August to 14 September, 2007 in the South China Sea. The sites within the two circles indicate the stations where the *P-E* curves were established.

Experimentation. To determine the photosynthetic carbon fixation under different radiation treatments, water samples were prefiltered through 180 μm pore-size-mesh, dispensed into 50 mL quartz or glass tubes and inoculated with $NaH^{14}CO_3$ solution before being incubated under the radiation treatments with or without UV (see below).

Additionally, the photosynthesis vs PAR (*P-E*) relationship was established in the absence or presence of UVR in both off-shore and near-shore areas (Fig. 1). Such *P-E* curves were based on the data obtained on August 16, 17, 20, 21 and September 2, 5, 7. A total of 9 or 10 levels of natural radiation (*i.e.* from 100 to $<2\%$) were achieved by covering the samples with none or an increasing number of neutral density screens.

Radiation treatments and measurements. Triplicate samples were exposed to each of three different radiation treatments: (1) samples receiving the full spectrum of solar radiation (PAB, PAR + UV-A + B) unwrapped quartz tubes; (2) samples receiving the irradiance above 325 nm (PA, PAR + UV-A) uncovered glass tubes (50% cutoff at 325 nm); and (c) samples receiving the irradiance above 395 nm (P, PAR) quartz tubes wrapped with Ultraphan 395 foil (UV Opak, Digefra, Munich, Germany). The transmission spectra of the tubes and cut-off foil are shown in Fig. 2. All the tubes containing the water sample were incubated for 6 h (9:00–15:00) beneath the surface (5 cm) in a water bath in which the temperature was controlled within a range of 27–30°C (the same range as the SST) by continuously pumped surface seawater. Duplicate tubes wrapped in aluminum foil were incubated as dark controls. A total of 32 incubations were performed during the cruise.

The incident solar radiation was continuously monitored using an Eldonet broadband filter radiometer (Eldonet XP, Real Time Computer, Möhrendorf, Germany) that was fixed at the top of the ship. This device has three channels for PAR (400–700 nm), UV-A (315–400 nm) and UV-B (280–315 nm) irradiance, respectively (32). It measures the solar irradiances and records the means over each minute, and was calibrated regularly with the support from the maker against a double monochromator spectroradiometer and a certified calibration lamp. Since the glass cuts off UV-B and parts of the UV-A (315–325 nm) wavebands, water samples in the glass tubes received about 5% less UV-A irradiance as compared with the measured value.

Determination of photosynthetic carbon fixation. Prefiltered (180 μm pore-size) water samples were dispensed into 50 mL tubes, inoculated with 100 μL of 5 μCi (0.185 MBq) $NaH^{14}CO_3$ solution (ICN Radiochemicals, USA) and incubated under the conditions described above. After the incubations, the cells were filtered onto a Whatman GF/F glass fiber filter (25 mm), which was immediately frozen and stored at −20°C for later analysis. The frozen filter was placed into a 20 mL scintillation vial, thawed and exposed to HCl fumes overnight and dried (55°C, 6 h) to expel nonfixed ^{14}C. After this, 3 mL scintillation cocktail (Perkin Elmer®) was added to each vial and the radioactivity was counted with a liquid scintillation counter (LS 6500, Beckman Coulter, USA). The photosynthetic carbon fixation was determined according to Holm–Hansen and Helbling (33).

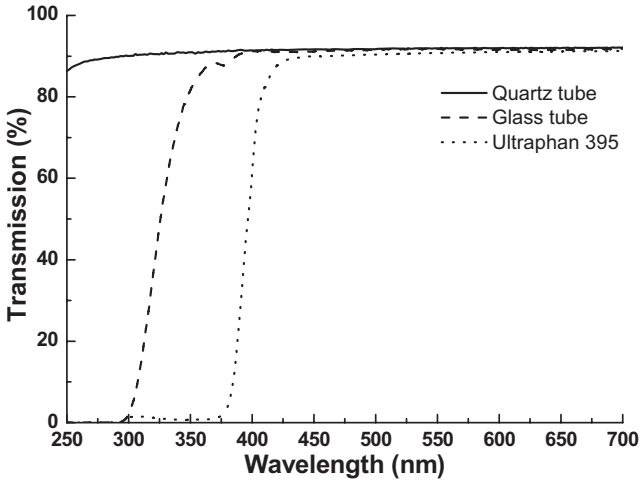

Figure 2. Transmission spectra (in %) of the quartz, glass tubes and Ultraphan 395 UV-cut off filter.

Chlorophyll a and species analyses. At the beginning of each experiment, chlorophyll *a* (chl *a*) concentration was determined by filtering 3–4 L of surface seawater onto a Whatman GF/F glass fiber filter (25 mm), which was then wrapped with aluminum foil and stored at −20°C for later extraction and measurement. Chl *a* concentration was determined spectrophotometrically with a scanning spectrophotometer (UV 2501-PC, Shimadzu, Japan) following the equations of Porra (34) after complete extraction in 5 mL absolute methanol. For the piconanoplankton fraction, a subsample was prefiltered through a Nitex® mesh (20 μm), and the chl *a* concentration was determined as described above.

For species analysis, phytoplankton samples were fixed with buffered formalin (final concentration of 0.4%). After the cells had settled in a 50 mL cylinder of Utermöhl Chamber (Hydro-Bios, Germany) for 24 h, qualitative and quantitative analyses were carried out with an inverted microscope (IX51, OLYMPUS, Japan) according to Villafañe and Reid (35).

Data analysis. The *P* vs *E* curves were analyzed using the model of Eilers and Peeters (36) and fitting the data by iteration: $P^B = E/(aE^2 + bE + c)$, where P^B is the photosynthetic rate [μg C (μg chl *a*)$^{-1}$ h^{-1}], *E* is the irradiance (W m^{-2}), and *a*, *b*, and *c* are the adjustment parameters. Since the uncovered quartz or glass tubes received 4% higher PAR than those covered with Ultraphan 395 filters under water, the PAR values were calibrated by multiplying by 0.96 for the *P* vs *E* curves with the cut-off filters (14). The daily photosynthetic production in the surface seawater was estimated by integrating the measured rate of photosynthesis at different light levels over the daytime (37):

$$\sum \mathrm{PP} = \int_{t=\mathrm{sunrise}}^{\mathrm{sunset}} \mathrm{PAR}(t)/(a \times \mathrm{PAR}^2(t) + b \times \mathrm{PAR}t + c) \times [\mathrm{chl}a],$$

where $\sum$PP represents the daily carbon fixation (μg C L^{-1} day^{-1}); *a, b* and *c* are the adjustment parameters described above, whereas (chl *a*) represents the chl *a* concentration (μg L^{-1}). UVR-induced inhibition on photosynthetic carbon fixation or daily photosynthetic production was calculated as follows: Inh-A (%) = $(P_P - P_{PA})/P_P \times 100\%$, Inh-B (%) = $(P_{PA} - P_{PAB})/P_P \times 100\%$, where Inh-A or B represent the inhibition caused by UV-A or B, whereas the UVR-Inh is the sum of Inh-A and B; P_P, P_{PA} and P_{PAB} the carbon fixation or daily photosynthetic production under PAR-alone, PAR + UV-A and PAR + UV-A + B treatments, respectively.

One-way ANOVA or paired *t*-test was used to establish significant differences between the treatments. The correlation analyses between variables were established using a Kendall's τ test with 95% confidence limit; and a power function ($Y = A\,x^B$) was used to fit the data, where A and B are coefficients and x is the distance off the coasts.

RESULTS

During the cruise, the daily dose of UV-B irradiance varied between 18.4 and 69.2 KJ m^{-2}, that of UV-A between 0.5 and 1.85 MJ m^{-2}, and that of PAR ranged from 3.14 to 13.1 MJ m^{-2} (Fig. 3). The average ratio of UV-B to PAR ranged from 0.52% to 0.61%; whereas that of UV-A to PAR from 13.8% to 15.9%. Changes in the cloud cover were the reason for the variation. The ozone column concentration over the monitored area varied from 259 to 276 D.U. during the period (data obtained from: http://jwocky.gsfc.nasa.gov/), that negatively correlated with the measured UV-B irradiance or UV-B to PAR ratio. Surface seawater temperature (SST) and salinity (SSS) ranged from 26 to 30°C and 32 to 34, within the upper mixed layer (UML) varying from 40 to 50 m. The euphotic zone was about 75 to 80 m deep for the investigated areas, and UV-A and UV-B (1% surface irradiance) penetrated up to 49–54 m and 28–33 m, respectively.

Chlorophyll *a* concentration in surface seawater changed spatially from 0.32 to 0.10 μg L^{-1}, with the highest value in the coastal and the lowest in the pelagic waters (Fig. 4A). The maximal and minimal concentrations of chl *a* were observed at sites 46 and 650 km off the coasts, respectively; the high chl *a* levels were associated with high proportions of microplankton (> 20 μm) (Fig. 4A). With increasing distance from the coast toward the pelagic area, phytoplankton biomass (chl *a*) decreased drastically, while the proportion of chl *a* in piconanoplankton fraction (< 20 μm) increased significantly ($P < 0.05$) (Fig. 4A). Microscopic phytoplankton, mainly diatoms (*e.g.*, *Chaetoceros* sp., *Thalassionema* sp. and *Skeletonema costatum*), were the dominant species in the coastal waters; whereas unidentified monads or flagellates were the most abundant groups in the pelagic waters. Few microplankton cells in addition to *Trichodesmium* sp. were observed in the open waters, however, microscopic diatoms were occasionally found at the stations (*e.g.* 14ºN, 112ºE) near the cold eddy.

The photosynthetic carbon fixation rate decreased from the coastal to pelagic areas either based on chl *a* or per volume of seawater (Fig. 4B,C). The rate per volume of seawater under PAR-alone treatment around local noon period ranged from 2.32 (near-shore) to 0.28 (off-shore) μg C L^{-1} h^{-1} (Fig. 4B); and the assimilation number varied from 7.31 (near-shore) to 2.44 (off-shore) μg C μg (chl *a*)$^{-1}$ h^{-1} (Fig. 4C). Under the full spectrum of solar radiation with the presence of UV, the photosynthetic carbon fixation was significantly reduced,

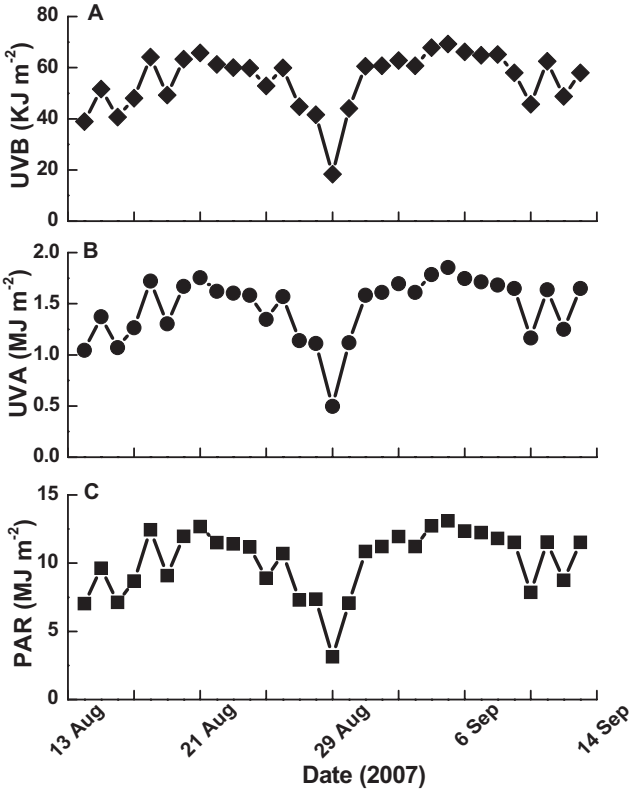

Figure 3. Daily doses of UV-B (280–315 nm), UV-A (315–400 nm) and PAR (400–700 nm) measured on the deck during the cruise.

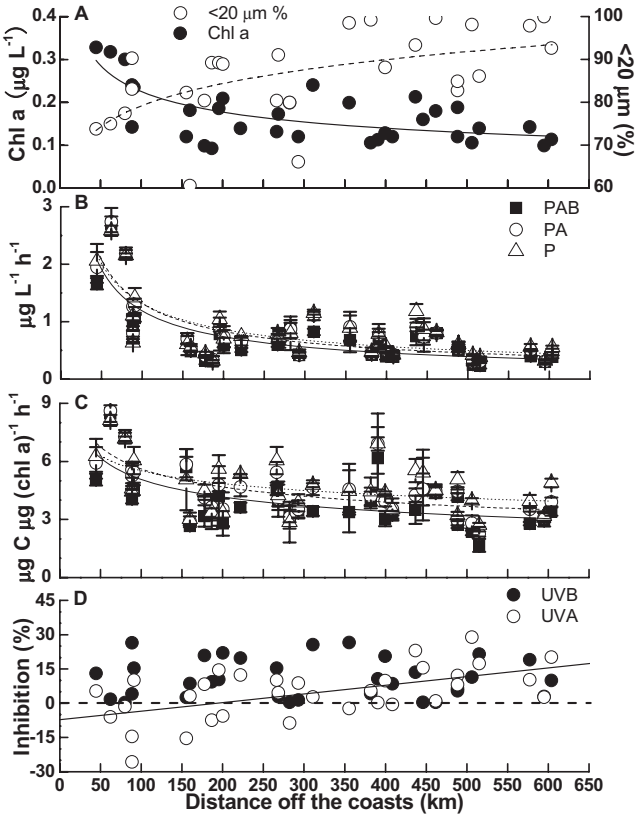

Figure 4. Variations of biological characteristics in surface seawater from the coasts to pelagic waters of the SCS. (A) Phytoplankton biomass (chl *a*, in μg L^{-1}) and piconanoplankton fractions (< 20 μm, in %); the fitted lines are power functions ($Y = A\,x^B$, $R^2 = 0.47$ for chl *a* and 0.32 for piconano-fractions); (B) and (C) Photosynthetic carbon fixation rates per volume of seawater (in μg C L^{-1} h^{-1}) or based on chl *a* [in μg C (μg chl *a*)$^{-1}$ h^{-1}] under PAR (P), PAR + UVA (PA) or PAR + UVA + B (PAB); the fitted lines are the power functions ($R^2 = 0.38$–0.63); (D) Photosynthetic inhibition (in %) induced by UV-A or UV-B, the solid line indicates the significant relationship between the UV-A-induced inhibition and the distance off the coast ($R^2 = 0.31$, $P < 0.01$, $n = 32$). Vertical bars present the standard deviations ($n = 3$).

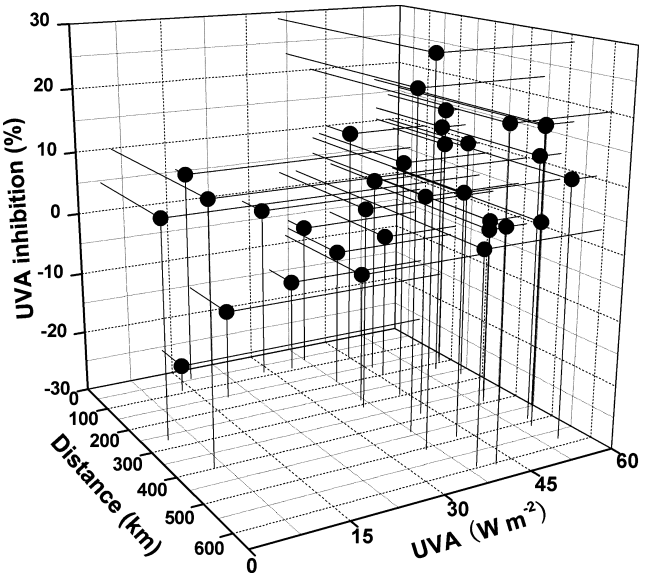

Figure 5. UV-A-induced inhibition (in %) of the photosynthetic carbon fixation as a function of the mean irradiance (in W m^{-2}) during the incubation and the distance (in km) off the coasts.

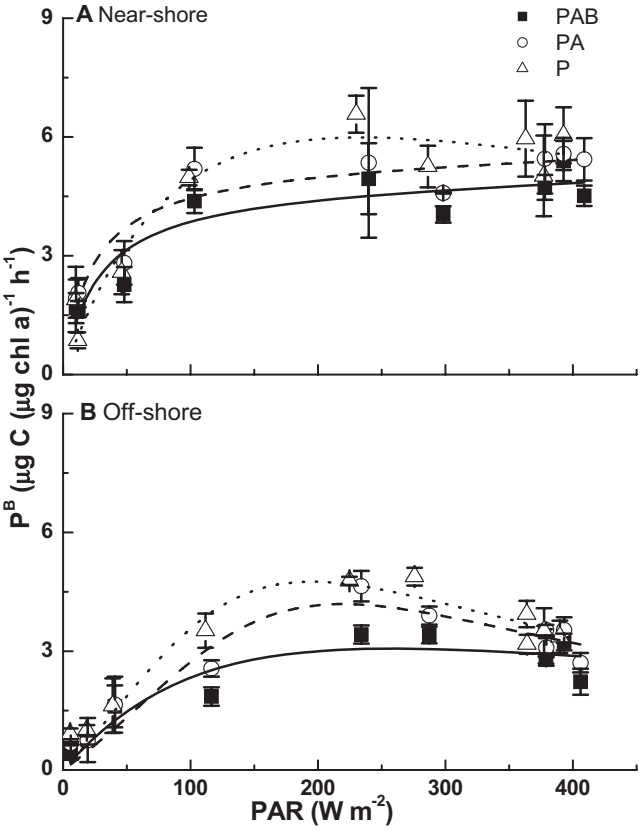

Figure 6. Phytoplankton assimilation number [in μg C (μg chl *a*)$^{-1}$ h^{-1}] as function of PAR irradiance (in W m^{-2}) from (A) the near-shore or (B) the off-shore water (see Fig. 1). The surface seawater was exposed to PAB (280–700 nm), PA (320–700 nm) and P (400–700 nm) treatments during August 16, 17, 20, 21 and September 2, 5 and 7, respectively. R^2 values of the *P* vs *E* curves ranged from 0.86 to 0.92 (n = 27 or 30); whereas the vertical bars represent the standard deviations (n = 3).

compared with the PAR-alone treatment (Fig. 4B,C). The inhibition ranged from −25% to 28.9% for UV-A and from 0.34% to 26.5% for UV-B (Fig. 4D). The negative value of UV-A-induced inhibition reflects the enhanced photosynthesis caused by moderate levels of UV-A, which was merely observed in the near-shore waters (*e.g.* <200 km off the coast) where micro-cells were abundant (Fig. 5). The UV-A related inhibition increased from the coastal to pelagic waters, whereas UV-B impacted uniformly throughout the period and over the distance (Fig. 4D).

When the relationships of the photosynthetic carbon fixation rate with PAR levels (*P* vs *E* curves) were established with or without UV, significant differences in UVR-induced impacts were also found from the near-shore to off-shore waters (Fig. 6). At reduced levels of solar radiation, UV-A-induced enhancement of the photosynthetic carbon fixation was detected in the near-shore water, as reflected by the higher rate in the presence of UV compared with PAR-alone treatment (P) (Fig. 6A). Daily photosynthetic production per volume of seawater (PAR-alone) was 15.7 μg C L^{-1} day^{-1} in the near-shore and 4.65 μg C L^{-1} day^{-1} in the off-shore water, with the former more than three times higher than the later (Fig. 7A). When based on chl *a*, it was 52.7 and 33.5 μg C (μg chl *a*)$^{-1}$ day^{-1} for the near- and off-shore water, respectively (Fig. 7B). The inhibition of daily primary production caused by UV in surface seawater was about 20.8% and 26.7% in the near- and off-shore areas, respectively; UV-A caused 4.26% in near-shore and 13.2% in off-shore, while UV-B caused 16.5% in near- and 13.5% in off-shore surface waters, respectively (Fig. 7C). UV-A caused more damage to the phytoplankton cells in the offshore surface seawater.

DISCUSSION

In this study, we demonstrated the effects of solar UV on photosynthetic carbon fixation in surface seawater over 250 000 km^2 in the SCS. With increasing distance from the coast, drastic decreases were observed in "chl *a*" concentration and CO_2 fixation rate either based on chl *a* or per volume of seawater. UV-A-induced photoinhibition of photosynthesis increased with increasing distance from the coast, while UV-B decreased the carbon fixation almost equally over the distance. Positive effects of UV-A under reduced levels of solar radiation were only found in the near shore seawaters where microplankton cells were abundant and on the days of reduced radiation.

Pelagic waters are usually oligotrophic and less productive (23,27); whereas coastal waters are often more productive due to higher availability of nutrients derived from the runoffs or fishery activities (13,14,20,21). In the open oceans, the decrease in chl *a* concentration and photosynthetic rate (Fig. 4A–C) is known to be due to the limited availability of nutrients (18,19,23). On the other hand, the higher proportion of smaller cells (Fig. 4A) could also lead to lower photosynthetic production in the offshore waters (Fig. 4B), because they often have lower photosynthetic rates, as found in this study (Fig. 4C) and in others (38). The smaller cells can use nutrients more efficiently due to their larger surface to volume ratios (39), and thus successfully dominate the oligotrophic oceans. Additionally, large cells show lower susceptibility to

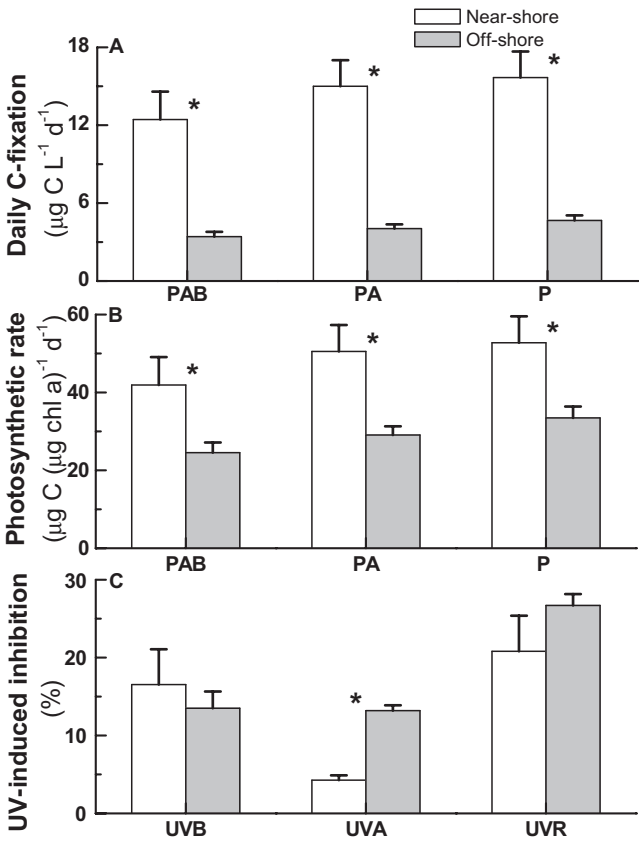

Figure 7. Integrated daily photosynthetic carbon fixation in the near and offshore waters on the basis of water volume [(A), in μg C L^{-1} day^{-1}]; or chl *a* [(B), in μg C (μg chl *a*)$^{-1}$ day^{-1}] under PAB (280–700 nm), PA (320–700 nm) or P (400–700 nm) treatments, and UV-induced inhibition (in %) of the daily photosynthetic production (C). The vertical bar represents the standard deviation (n = 3); whereas the stars (*) represent the significant differences ($P < 0.05$).

photoinactivation, and therefore incur lower costs to endure short-term exposures to high light or UV under frequently mixed waters (40).

In most of the stations, UVR significantly reduced the photosynthetic carbon fixation in the surface seawater (Fig. 4B,C). Taking into account the insufficient repair of UV-induced damage (41), the high inhibition caused by UV on the carbon fixation could be attributed to high solar radiation (Fig. 3) and less mixing in the SCS (28). The increase in UV-A induced inhibition from the coasts to pelagic oceans (Fig. 4D) might be caused by the changes in taxonomic structure (Fig. 4A). Picoplankton cells (<2 μm) are more sensitive to UV in view of their DNA damage or physiological responses (7,26,30). In addition, less nutrient availability can also lead to higher sensitivity to UV (42). On the other hand, moderate levels of UV-A enhanced the carbon fixation by phytoplankton cells, though it only occurred in the near-shore areas (Fig. 5) where micro-cells (>20 μm) are plentiful (Fig. 4A). Such an UV-A utilization for photosynthesis has been previously demonstrated in coastal water (13,14). However, UV-A did not bring any enhancement of the carbon fixation in pelagic water (Fig. 5) where picophytoplankton-dominated assemblages from the oligotrophic water (Fig. 4A) are not optically efficient in synthesizing and UVACs (24,25); whereas the cells in coastal waters were shown to accumulate the UVACs that have been suggested to aid in the utilization of UV-A energy (14). UV-stimulated inorganic carbon acquisition has also been observed in phytoplankton species (43,44). On the other hand, phytoplankton cells grown in nutrient replete conditions were more resistant to solar UVR while their contents of UVACs increased (29). Consequently, the combination of UV-A-induced positive effects and higher tolerance of UV led to lower UV-induced inhibition of the assimilation number in the coastal water of the SCS.

Considering the spatially disparate UV-induced positive and negative impacts and the considerable depth (up to 60 m) that UV can penetrate, total carbon fixation for the euphotic zone tends to be underestimated in coastal water if solar UVR was not considered (14); for offshore waters, where UV-A-stimulated photosynthetic carbon fixation was not observed and higher photoinhibition was caused by UVR, daily photosynthetic production could have been overestimated without considering the effects of UVR (Figs. 6B and 7).

Acknowledgements—We are thankful for the comments and suggestions of two anonymous reviewers and of the Associate Editor that helped to improve our manuscript. This work was supported by National Basic Research Program of China (No. 2009CB421207), National Natural Science Foundation (No. 40930846, No. 40876058) and Changjiang Scholars and Innovative Research Team Program (IRT0941). We are also grateful to the members of PCSIRT group and all the crews on Dong Fang Hong II Ship for their experimental assistance.

REFERENCES

1. Smith, R. C. and K. S. Baker (1979) Penetration of UV-B and biologically effective dose-rates in natural waters. *Photochem. Photobiol.* **29**, 311–323.
2. Häder, D. P., H. D. Kumar, R. C. Smith and R. C. Worrest (2007) Effects of solar UV radiation on aquatic ecosystems and interactions with climate change. *Photochem. Photobiol. Sci.* **6**, 267–285.
3. Behrenfeld, M., J. Hardy, H. Gucinski, A. Hanneman, H. Lee and A. Wones (1993) Effects of ultraviolet-B radiation on primary production along latitudinal transects in the south Pacific Ocean. *Mar. Environ. Res.* **35**, 349–363.
4. Litchman, E. and P. J. Neale (2005) UV effects on photosynthesis, growth and acclimation of an estuarine diatom and cryptomonad. *Mar. Ecol. Prog. Ser.* **300**, 53–62.
5. Sobrino, C., O. Montero and L. M. Lubián (2004) UV-B radiation increases cell permeability and damages nitrogen incorporation mechanisms in *Nannochloropsis gaditana*. *Aquat. Sci.* **66**, 421–429.
6. Sass, L., C. Spetea, Z. Máté, F. Nagy and I. Vass (1997) Repair of UV-B induced damage of photosystem II via de novo synthesis of the D1 and D2 reaction centre subunits of *Scynechocystis* sp. PCC 6803. *Photosynth. Res.* **54**, 55–62.
7. Helbling, E. W., A. G. J. Buma, M. K. de Boer and V. E. Villafañe (2001) In situ impact of solar ultraviolet radiation on photosynthesis and DNA in temperate marine phytoplankton. *Mar. Ecol. Prog. Ser.* **211**, 43–49.
8. Buma, A. G. J., P. Boelen and W. H. Jeffrey (2003) UVR-induced DNA damage in aquatic organisms. In *UV Effects in Aquatic Organisms and Ecosystems* (Edited by E. W. Helbling and H. E. Zagarese), pp. 291–327. The Royal Society of Chemistry, Cambridge.
9. Gao, K., P. Li, T. Watanabe and E. W. Helbling (2008) Combined effects of ultraviolet radiation and temperature on morphology,

photosynthesis, and DNA of *Arthrospira* (spirulina) *platensis* (Cyanophyta). *J. Phycol.* **44**, 777–786.
10. Agustí, S. and M. Llabrés (2007) Solar radiation-induced mortality of marine pico-phytoplankton in the oligotrophic ocean. *Photochem. Photobiol.* **83**, 793–801.
11. Karentz, D., J. E. Cleaver and D. L. Mitchell (1991) Cell survival characteristics and molecular responses of Antarctic phytoplankton to ultraviolet-B radiation. *J. Phycol.* **27**, 326–341.
12. Mengelt, C. and B. B. Prézelin (2005) UVA enhancement of carbon fixation opens a potential ecological niche for the toxic diatom *Pseudo-nitzschia australis* in high UVR exposed surface waters. *Mar. Ecol. Prog. Ser.* **301**, 81–93.
13. Gao, K., G. Li, E. W. Helbling and V. E. Villafañe (2007a) Variability of UVR effects on photosynthesis of summer phytoplankton assemblages from a tropical coastal area of the South China Sea. *Photochem. Photobiol.* **83**, 802–809.
14. Gao, K., Y. Wu, G. Li, H. Wu, V. E. Villafañe and E. W. Helbling (2007b) Solar UV-radiation drives CO2-fixation in marine phytoplankton: A double-edged sword. *Plant Physiol.* **144**, 54–59.
15. Barbieri, E. S., V. E. Villafañe and E. W. Helbling (2002) Experimental assessment of UV effects upon temperate marine phytoplankton when exposed to variable radiation regimes. *Limnol. Oceanogr.* **47**, 1648–1655.
16. Helbling, E. W, K. Gao, R. J. Gonçalves, H. Wu and V. E. Villafañe (2003) Utilization of solar UV radiation by coastal phytoplankton assemblages off SE China when exposed to fast mixing. *Mar. Ecol. Prog. Ser.* **259**, 59–66.
17. Halldal, P. (1967) Ultraviolet action spectra in algology: A review. *Photochem. Photobiol.* **6**, 445–460.
18. Le Bouteiller, A., J. Blanchot and M. Rodier (1992) Size distribution patterns of phytoplankton in western Pacific: Towards a generalization for the tropical open ocean. *Deep-Sea Res.* **39**, 805–823.
19. Marañón, E., P. M. Holligan, R. Barciela, N. González, B. Mouriño, M. J. Pazló and M. Varela (2001) Patterns of phytoplankton size structure and productivity in contrasting open-ocean environments. *Mar. Ecol. Prog. Ser.* **216**, 43–56.
20. Shen, Z. (2001) Historical changes in nutrient structure and its influences on phytoplankton composition in Jiaozhou Bay. *Estuar. Coast. Shelf S.* **52**, 211–224.
21. Ho, A. Y. T., J. Xu, K. Yin, X. Yuan, L. He, Y. Jiang, J. H. W. Lee, D. M. Anderson and P. J. Harrison (2008) Seasonal and spatial dynamics of nutrients and phytoplankton biomass in Victoria Harbour and its vicinity before and after sewage abatement. *Mar. Pollut. Bull.* **57**, 313–324.
22. Kolber, Z., K. D. Wyman and P. G. Falkowski (1990) Natural variability in photosynthetic energy conversion efficiency: A field study in the Gulf of Maine. *Limnol. Oceanogr.* **35**, 72–79.
23. Falkowski, P. G., M. Koblížek, M. Gorbunov and Z. Kolber (2004) Development and application of variable chlorophyll fluoresence techniques in marine ecosystems. In *Chlorophyll a Fluorescence: A Signature of Photosynthesis* (Edited by G. C. Papageorgiou and Govindjee), pp. 757–778. Springer, the Netherlands.
24. Raven, J. A. (1991) Responses of photosynthetic organisms to increased solar UV-B. *J. Photochem. Photobiol. B Biol.* **9**, 239–244.
25. Garcia-Pichel, F. (1994) A model for internal self-shading in planktonic organisms and its implications for the usefulness of ultraviolet sunscreen. *Limnol. Oceanogr.* **39**, 1704–1717.
26. Callieri, C., G. Morabito, Y. Huot, P. J. Neale and E. Litchman (2001) Photosynthetic response of pico- and nanoplanktonic algae to UVB, UVA and PAR in a high mountain lake. *Aquat. Sci.* **63**, 286–293.
27. Tseng, C. M., G. T. F. Wong, I. I. Lin, C. R. Wu and K. K. Liu (2005) A unique seasonal pattern in phytoplankton biomass in low-latitude waters in the South China Sea. *Geophys. Res. Lett.* **32**, L08608.
28. Chen, C. C., F. K. Shiah, S. W. Chung and K. K. Liu (2006) Winter phytoplankton blooms in the shallow mixed layer of the South China Sea enhanced by upwelling. *J. Marine Syst.* **59**, 97–110.
29. Marcoval, M. A., V. E. Villafañe and E. W. Helbling (2008) Combined effects of solar ultraviolet radiation and nutrients addition on growth, biomass and taxonomic composition of coastal marine phytoplankton communities of Patagonia. *J. Photochem. Photobiol. B Biol.* **91**, 157–166.
30. Li, G., Y. Wu and K. Gao (2009) Effects of typhoon Kaemi on coastal phytoplankton assemblages in the South China Sea, with special reference to the effects of solar UV radiation. *J. Geophys. Res.* **114**, G04029
31. Wu, Y., K. Gao, G. Li and E.W. Helbling (2010) Seasonal impacts of solar UV radiation on the photosynthesis of phytoplankton assemblages in the coastal water of the South China Sea. *Photochem. Photobiol.* **86**, 586–592.
32. Häder, D. P., M. Lebert, R. Marangoni and G. Colombetti (1999) ELDONET – European Light Dosimeter Network hardware and software. *J. Photochem. Photobiol. B Biol.* **52**, 51–58.
33. Holm-Hansen, O. and E. W. Helbling (1995) Técnicas para la medición de la productividad primaria en el fitoplancton. In *Manual de Métodos Ficológicos* (Edited by K. Alveal, M. E. Ferrario, E. C. Oliveira and E. Sar), pp. 329–350. Universidad de Concepción, Concepción, Chile.
34. Porra, R. J. (2002) The chequered history of the development and use of simultaneous equations for the accurate determination of chlorophylls a and b. *Photosynth. Res.* **73**, 149–156.
35. Villafañe, V. E. and F. M. H. Reid (1995) Métodos de microscopía para la cuantificación del fitoplancton. In *Manual de Métodos Ficológicos* (Edited by K. Alveal, M. E. Ferrario, E. C. Oliveira and E. Sar), pp. 169–185. Universidad de Concepción, Concepción, Chile.
36. Eilers, P. H. C. and J. C. H. Peeters (1988) A model for the relationship between light intensity and the rate of photosynthesis in phytoplankton. *Ecol. Model* **42**, 199–215.
37. Behrenfeld, M. J. and P. G. Falkowski (1997) A consumer's guide to phytoplankton primary productivity models. *Limnol. Oceanogr.* **42**, 1479–1491.
38. Fernández, E., E. Marañón, X. A. G. Morán and P. Serret (2003) Potential causes for the unequal contribution of picophytoplankton to total biomass and productivity in oligotrophic waters. *Mar. Ecol. Prog. Ser.* **254**, 101–109.
39. Raven, J. A. and J. E. Kübler (2002) New light on the scaling of metabolic rate with the size of algae. *J. Phycol.* **38**, 11–16.
40. Key, T., A. McCarthy, D.A. Campbell, C. Six, S. Roy and Z.V. Finkel (2010) Cell size trade-offs govern light exploitation strategies in marine phytoplankton. *Environ. Microbiol.* **12**, 95–104.
41. Neale, P. J., E. W. Helbling and H. E. Zagarese (2003) Modulation of UVR exposure and effects by vertical mixing and advection. In *UV Effects in Aquatic Organisms and Ecosystems* (Edited by E. W. Helbling and H. E. Zagarese), pp. 107–134. The Royal Society of Chemistry, Cambridge.
42. Litchman, E., P. J. Neale and A. T. Banaszak (2002) Increased sensitivity to ultraviolet radiation in nitrogen-limited dinoflagellates: Photoprotection and repair. *Liminol. Oceanogr.* **47**, 86–94.
43. Beardall, J., C. Sobrino and S. Stojkovic (2009) Interactions between the impacts of ultraviolet radiation, elevated CO_2, and nutrient limitation on marine primary producers. *Photochem. Photobiol. Sci.* **8**, 1257–1265.
44. Wu, H. and K. Gao (2009) UV radiation-stimulated activity of extracellular carbonic anhydrase in the marine diatom *Skeletonema costatum*. *Funct. Plant Biol.* **36**, 137–143.